UCLA
UCLA Electronic Theses and Dissertations

**Title**
Suppression of ADAM23 is functionally associated with HPV-mediated carcinogenesis

**Permalink**
https://escholarship.org/uc/item/3w3819v6

**Author**
Yang, Paul

**Publication Date**
2017

Peer reviewed|Thesis/dissertation

eScholarship.org Powered by the California Digital Library
University of California

UNIVERSITY OF CALIFORNIA

Los Angeles

# Suppression of ADAM23 is functionally associated with HPV-mediated carcinogenesis

A thesis submitted in partial satisfaction

of the requirements of the degree Master of Science

in Oral Biology

by

Paul Yang

2017

ABSTRACT OF THESIS

ADAM23 plays functional role in HPV-associated cancer development

By

Paul Yang

Master of Science in Oral Biology

University of California, Los Angeles 2017

Professor Reuben Han-Kyu Kim, Chair

Professor Mo K Kang

Professor Yong Kim

Human Papilloma Virus (HPV) mediated Oropharyngeal Squamous Carcinoma (OPSC) is becoming more relevant and alarming as oral exposure to HPV is increasing. HPV is a DNA virus that infects keratinocytes found in the epithelia of oral cavity. HPV genome translocation to the host nucleus and subsequent expression of oncoproteins E6 and E7 is a hallmark in development of HPV positive OPSCC. E6 allows a cell to bypass p53 regulation, and E7's interaction with pRb allows progression of cell cycle despite abnormalities, ultimately, permitting proliferation. However, HPV infection alone does not trigger malignant transformation as supported by the fact that only a few individuals with persistent HPV infection develop carcinoma. Therefore, we believe that additional genetic alteration or epigenetic regulation must take place to create an environment favorable for malignant transformation and

lead to development of cancer. We utilized human oral keratinocyte-16B (HOK-16B), a non-transformed oral keratinocyte harboring HPV-16 genome, and high-throughput RNAi Decode Library to create an event that may alter the phenotype of HOK-16B. We have identified and confirmed A Disintegrin And Metalloproteinase 23 (ADAM23) silencing in HOK-16B results in high cell proliferation rate. It also increases tumorigenic potential *in vitro* tumor sphere assay and anchorage independent soft agar assay. Furthermore, its increased tumorigenic potential led to formation of cyst *in vivo* xenograft experiment with immuncompromised mice. Microarray analysis of HOK-16B with ADAM23 silenced showed that several genes were upregulated, prominently, CLDN-1, which plays a critical role in cell-cell interaction, and metastasis in aggressive breast cancers. In addition, attenuating E6 or/and E7 expression in ADAM23 knocked-down HOK-16B showed, ADAM23 cooperates with these oncoproteins to enhance tumorigenic potential of HOK-16B. Furthermore, diminished expression of ADAM23 in HPV positive HNSCC supports the silence of ADAM23 and co-expression of E6 and E7 would lead to malignant transformation. These findings imply that ADAM23 could be useful therapeutic and prognostic marker screening individuals in high-risk of developing HPV positive HNSCC.

The thesis of Paul Yang is approved.

Reuben Han-Kyu Kim - Chair

Mo K Kang

Yong Kim

University of California, Los Angeles

2017

TABLE OF CONTENTS

## 1. INTRODUCTION

It has been reported that increasing number of malignancies are associated either directly or indirectly with viral infection. Increasing evidence suggests that production of viral genes following infection alters and modifies the growth-signaling pathway in an affected cell. This alteration can easily lead to unregulated proliferation making the infected cell cancerous.

While there are many different types of virus that can give rise to malignant cell types, Human Papillomavirus (HPV) is one of the most well-known types of cancer causing virus. It is one of the most common sexually transmitted infections worldwide and associated with development of cancer.

HPV is a small, DNA virus belonging to the papillomavirus family. It is 55 nanometers[1] in size, and contains approximately 8000 nucleotide base pairs[2,3]. Its genome encoded early structural genes (E1-E8) as well late structural genes (L1 and L2). Furthermore, it has been shown that early structural genes are responsible for malignant transformation. There are over 200 types of HPV identified, and about 30 types are known to be transmitted through sexual contact[3]. The virus is known for its unique establishment of infections only in keratinocytes of the skin or mucosal membrane, and its life cycle is dependent on the host cell's differentiation program.

HPV gains entry to the host keratinocyte through micro-abrasions after binding to putative receptors present on the host cell membrane. This allows the virus to enter the host via endocytosis. Following its entry, HPV genome enters the host nucleus and becomes established via an unknown mechanism. It has been shown that usually 10-200 viral genomes are present in

the infected cells. As the host keratinocyte undergoes differentiation, HPV genomes also become replicated and proceed toward the upper layers of the epithelium in the host.

HPV can be categorized into high-risk group and low-risk group. It has been suggested that persistent infection with the high-risk virion increases the chance of developing cancers of cervix, vulva, vagina, penis, oropharynx as well as anus. HPV 16 and HPV 18 are two types that account for 70% of cervical cancer cases. The molecular biology behind HPV-induced carcinogenesis has been well-studied and established using cervical cancer model.

Oncoproteins E6 and E7 are key players in HPV positive cancer development. Both proteins are known to hinder the proper regulation of host cell proliferation by interacting with well-known tumor suppressors p53 and pRb respectively. E6 interacts with p53. p53 is activated when DNA damage or abnormality in cell cycle is detected. p53 then causes either cell cycle arrest or cause apoptosis of the cell. However, in the presence of E6 oncoprotein, E6 forms a complex with p53 along with E6 associated protein. This complex ubiquitinates p53 marking it for proteosomal degradation. With p53 destroyed, the cell will continue its proliferation and therefore, propagation of HPV genome.

E7 shares similar mechanism with E6. E7 is known to interact with pRb, another putative tumor suppressor gene important for regulating G1/S and G2/M transitions in the cell cycle. When E7 binds pRb, it releases a transcription factor, $E2F^4$, which is important for activating downstream genes related to cell proliferation such as Cyclin A, E, and Cyclin-dependent kinase such as p21 and p27. With the transcription of these genes, the infected keratinocyte can continue to survive.

Most of our knowledge about HPV has been borrowed from the cervical cancer, and recently, general noticeable decline of HPV associated cervical cancer is observed due to

education and availability of vaccines. However, HPV positive with head and neck squamous cell carcinoma (HNSCC) is on the rise. More than 11,700 HPV related orophayngeal squamous cell carcinoma cases are reported annually in U.S.,[4] and contributes to substantial amount of cancer morbidity worldwide[5]. Historically speaking, major risk factors of HNSCC were smoking, tobacco, betel nut chewing and alcohol consumption[4]. However, we continue to see the increase in HNSCC despite decline in alcohol consumption, and 20-30% of HNSCC patients may not have these risky behaviors at all. A study by Gillison et al[6] attributes this finding to increased oral sex and oral exposure to HPV. Their study also demonstrated that HPV-positive HNSCC incidence was predominantly higher in young males of all races[6]. This clearly demonstrates that HPV associated HNSCC displays unique epidemiological features.

HPV-positive HNSCC also shows distinct clinical feature as well. Currently protocol for managing positive HPV-positive OPSCC involves a wide range of options from radiotherapy to removal of malignant tumors via surgery. The treatment plan is chosen based on the stage of the cancer as well as patient's age. Furthermore, it has been demonstrated that HPV harboring OPSCC shows better response to these therapies compared to HPV-negative OPSCC for an unexplained reason.

Due to these unique epidemiological and clinical features associated with HPV mediated OPSCC, it may not seem like an immediate threat. However, considering unique demographic group suffers from this viral infection due to constantly changing sexual behaviors, including increased oral sex, life number of sexual partners as well as sexual debut at younger age, it is suggested that those individuals suffer from HPV-positive HNSCC cancer is expected to surpass the annual number of cervical cancers by the year 2020[6]. This calls for development of unique

prognosis method that would allow rapid, early detection and intervention of this deadly viral infection.

The key mechanism behind malignant transformation, as mentioned, earlier includes incorporation of HPV genome and subsequent expression of oncoproteins E6 and E7. However, this genomic integration does not prescribe immediate arise of malignancy and development into cancerous phenotype. In fact, every sexually active individual will contract HPV at some point during his or her reproductive period, and only a fraction of infected individuals will develop carcinogenesis mediated by HPV. To support this finding, a study suggests only 10% of infected individuals carry a high risk of developing HNSCC while 90% will naturally eliminate the disease. Considering Imiquimoid[7], a topical ointment to boost host's T-helper 1 immune response, as a treatment for the disease, it can be assumed a healthy individual with good immunity can easily rid of the infection and prevented from exposure to malignant transformation. Therefore, we believe in addition to E6 and E7 expression, other cellular alterations must take place in the affected cell to trigger arise in malignancy. We attribute additional genetic or epigenetic alteration may aggravate malignant transformation.

Historically, it is believed that cancerous tumor arises from a normal cell that undergone tumorigenic transformation following genetic mutations, and this transformed cell becomes the cell-of-origin for the tumor. This tumorigenic cell will then divide and maintain a population of self-renewing cancer stem cells (CSC) that can give arise to new tumorigenic cells or metastasize to different part of the body. While this is the most classically accepted notion behind cancer development, a recent paradigm shift includes disruption of epigenetic regulation as a cause in cancer development.

To investigate what other cellular alterations need to take place to yield HPV- mediated carcinogenesis favorable, we utilized HPV-16 harboring immortalized oral keratinocytes (HOK-16B) and high-throughput Decode RNAi Viral Screening Library (Thermo Scientific Open Biosystems). This, in a way, introduced an additional alteration to the cellular processes that take place in HPV-16 harboring keratinocyte. The viral pool contains microRNA-adapted shRNA (shRNAmir) capable of producing stable loss-of-function phenotypes. Each viral pool contains about ~10,000 constructs that allow rapid and massive parallel screening. The Decode RNAi viral screening library also utilizes a unique "molecular barcode" for each hairpin allowing a user to identify exactly what changes have occurred in the transfected cell. Harnessing the power of this technology, we knocked out several genes in HOK-16B, and discovered a putative tumor suppressor, A Disintegrin And Metalloproteinase 23 (ADAM 23).

After discovering ADAM23 as a potential target gene, a specific shRNA sequence against to knock down expression of ADAM23, and experiments were conducted to see the phenotype of HOK-16B. Kocking down of ADAM23 from HOK-16B resulted in increased proliferative potential especially in the cell medium that is non-permissive for HOK-16B. In vitro investigations demonstrated ADAM23 knocked down HOK-16B cells gained tumorigenic potential. In vivo experiment of nude mice xenograft confirmed and supported in vitro finding. Furthermore, microarray analysis has shown knocking down ADAM23 from HOK-16B upregulated a wide range of genes related to cancer development. In conclusion, our study demonstrates suppression of ADAM23 works cooperatively with HPV oncoproteins E6 and E7 to drive malignant transformation of HOK-16B cells.

## 2. MATERIALS AND METHODS

### 2.1 RNAi Viral Screening

HPV-16 harboring immortalized, but non-transformed oral epithelial cells (HOK-16B) was infected with high-throughput Thermo Scientific Open Biosystems Decode RNAi Viral Screening Library. 2 x 10^5 cells of HOK-16B were plated a day before infection in Keratinocyte Growth Medium (Lonza). Upon reaching 60-70% confluency, the viral pools from Decode RNAi Viral library was used to infect the cells. The supplier's pGIPZ lentiviral particle was used for control. Puromycin was used as a selective marker for selecting successfully infected cells. Puromycin was added to the growth medium for about a week as a selective pressure. The successfully infected cells then were grown in Dulbecco's Modified Eagle Medium (DMEM) (Invitrogen) supplemented with 10% super calf serum (Gemini Bio-products) and 5 µg/ml Gentamycin aminoglycoside antibiotic (Invitrogen) for further selection and isolation of surviving colonies of HOK-16B cells.

### 2.2 Cells and cell culture

Surviving HOK-16B colonies after transfection were transferred in DMEM+10%SCS+5 µg/ml antibiotics, maintained, and proliferation curves were achieved. The cells were passed when 70% confluency achieved, and the population doubling was achieved at the time of passing. The cells were maintained for about 250 days. At the terminal stage of cell passage, the surviving colonies were stained with crystal violet to evaluate the proliferation potential. Another group of isolated HOK-16B colonies were grown and maintained in KGM as well following the same protocol.

### 2.3 Gene Identification

Survived HOK-16B colonies were trypsinzed and collected. Total Genomic DNA (gDNA) was isolated from the cells using DNeasy Blood & Tissue Kit (Qiagen). The quality of gDNA was assessed using NanoDrop Spectrophotometer (Thermo Fisher Scientific). Isolated gDNA was then used as a template for PCR amplification using a specific set of primers designed to flank the shRNAmir hairpin sequences provided with the Decode RNAi Viral Pools. Native *Taq* DNA Polymerase was used for PCR reaction. PCR amplicon was then confirmed on 1.2% agarose gel, and cloned into *E.coli* competent cells following the standard transformation protocol. *E.coli* plasmids were then isolated using Miniprep Kit (Qiagen) and sequenced by Laragen, Inc. (Culver City, CA).

### 2.4 Western Blotting

The following whole cell extracts were isolated using the lysis buffer (1% Triton X-100, 20mM Tris-HCl pH7.5, 150 mM NaCl, 1 mM EDTA, 2.5 mM sodium pyrophosphate, 1 μM β-glycerophosphate, 1 mM sodium orthovanadate, 1 mg/ml PMSF): 10-09 Normal Human Oral Keratinocytes (NHOK), 10-15 NHOK, SCC4 (HPV-), SCC9 (HPV-), SCC15 (HPV-), Tu139 (HPV-), Tu177 (HPV-) and FaDu (HPV-). HPV associated HOK-16B, BapT, CaSki, HeLa, SiHa's whole cell extracts were also isolated using the same lysis buffer. These extracts were run through 10% SDS-PAGE gel and transferred to protein membranes (Millipore, Billerica, MA). BenchMark Pre-stained Protein Ladder (Invitrogen) and MagicMark XP Western Protein Standard (Invitrogen) were mixed in 1:1 ratio and used as a protein ladder. The membranes were then blocked with 5% nonfat milk and incubated with the primary ADAM23 antibody (Abcam) overnight and secondary Anti-Rabbit-Horse radish peroxide (HRP) antibody (Santa Cruz) for 1.5

hrs. After antibody incubation, the membranes were exposed to the chemiluminescence reagent (Denville) for detection of proteins.

**2.5 Real-time quantitative RT-PCR (qRT-PCR)**

All qRT-PCR done in this study followed this protocol. Total RNA was isolated from cultured cells using TRIzol reagent (Invitrogen), and the quality of RNA was assessed using NanoDrop Spectrophotometer (Thermo Fisher Scientific). cDNA was generated from 5 µg of total RNA extracted using SuperScript first-strand synthesis system (Invitrogen). Then 2.5 ul cDNA was amplified using SYBR Green I Master Mix (Roche Applied Sciences) with the LightCycler 480 II real-time PCR system with primers. The primer sequences were obtained from the Universal Probe Library database. The cDNA samples were loaded in triplicates in LightCycler 96 well plates (Roche). GAPDH was used as internal control for the reaction. Second derivatives Cq values of the genes and GAPDH were compared to assess the fold-differences of amplification following the manufacturer's instruction (Roche).

**2.6 Knockdown of ADAM23 using shRNA 1-3**

To rule out the effects of other constructs of shRNA present in the pool conferring to the phonotypical changes observed, independent constructs of ADAM23 shRNAs 1-3 (Thermo Scientific) were used on HOK-16B cells. Identical procedures were followed to transfect the cells as mentioned previously. The expression of ADAM23 was assayed using qRT-PCR and Western Blotting; and cell proliferation was also determined. It has been shown that shRNA3 was the most effective copy of construct that attenuated the expression of ADAM23. Therefore, in the subsequent experiments, HOK-16B transfected with Construct 3 was used, and named HOK16B/ADAM23i.

### 2.7 Tumor Sphere Formation Assay

For us to evaluate the tumorigenic potential of ADAM23 knocked down HOK-16B in vitro, we utilized pGIPZ transfected HOK16B, a non-target control and HOK-16B/ADAM23i-3. 1000 cells per well were plated in Ultralow Cluster Plates (Fisher) and grown in tumor sphere medium (Serum Free DMEM/F12, 1x $N_2$ Supplement, 10ng/ml bFGF, and 10ng/ml EGF) for 7 days. Then tumor sphere cells were counted and their size was noted using Cell Sense software by Olympus Inc.

### 2.8 Anchorage Independent Soft Agar Assay

Soft agar assay was used to determine the colony-forming efficiency in semi-solid medium, 1 x $10^4$ of ADAM23 knocked down HOK-16B cells were seeded in 0.4% agarose containing DMEM. 0.8% DMEM agarose served as a base layer. Furthermore, pGIPZ transfected HOK16B cells were served as negative control, and ADAM23 knocked down HOK-16B cells grown in KGM was used as positive control. The cells were incubated for a week, and the colonies were counted. This assay was performed in triplicates with 12-well plates.

### 2.9 Organotypic Raft Cultures

HOK-16B/pGIPZ (control) and HOK-16B/ADAM23i cells were grown as organotypic raft cultures using techniques established previously [8]. $10^6$ cells were seeded on the submucosal equivalents consisting type I collagen and normal human oral fibroblasts. The cells were grown to confluence, submerged in the culture medium, and then exposed to the liquid-air interface by lowering the medium level. The medium contained DMEM/F12, Insulin (5 µg/ml), Hydrocortisone (0.4 µg/ml), Triiodo-thyronine (0.02 nM), Adenine (0.18 mM), Transferrin (5 µg/ml), Cholera toxin (0.1 nM), L-Glutamine (2 mM), 5% FBS, and Gentamycin (5 µg/ml). The

cultures were maintained in this “rafting” fashion for 14 days and were harvested by fixing in 10%

buffered formalin. Subsequently, hematoxylin-eosin (H&E) staining was performed on thick (6 μm) sagittal sections of each reconstructs to reveal the histological features. Sample processing, paraffin-embedding, sectioning, and H&E staining were performed at the UCLA’s Translational Pathology Core Laboratory (TPCL).

**2.9 Immunohistochemistry Staining**

Paraffin embedded OSC tissues were deparaffinized for 30 minutes in 60°C. The tissues were rehydrated by going through Xylene for 5 minutes, 100% ethanol for 1 minute, 95% ethanol for 1 minute and 70% ethanol for 1 minute. Then they were unmasked using citrated buffer in steam in >95°C for 25 minutes. To block endogenous peroxidase, the tissues were incubated with 3% hydrogen peroxide for 15 minutes. The tissue area was marked with Pap pen and incubated with 1X PBST for 5 minutes. 10% Blocking Buffer consists of Normal Goat Serum and PBST was using for 30 minutes. Then anti-ADAM23 (Sigma) (1:100) was diluted in 3-5% BSA, covered the tissue in a humid chamber for overnight in 4°C. The following day, the anti-rabbit (1:200)) was diluted in 3-5% BSA and covered the tissue for 40 minutes in the humid chamber. The tissue was then incubated with HRP-Avidin (Vector Laboratories) (1:1000) for 30 minutes, then the slide was developed using DAB solution for 2-5 minutes. Then hematoxylin was used to counter stain the tissue for 8 seconds, and dehydrated again by going through 70% ethanol for 1 minute, 95% ethanol for 1 minute, 100% ethanol for 1 minute and xylene for 3-5 minutes. Then the tissue was mounted with Permount and analyzed under microscope.

### 2.10 *In vivo* Tumor Formation Assay

Ten million cells of HOK-16B/pGIPZ, HOK-16B/ADAM23i-3 grown in KGM and DMEM+10% FBS were subcutaneously injected into the flank of immunocompromised mice (strain nu/nu, Charles River Laboratories). The animal study was performed according to the protocol approved by the UCLA Animal Research Committee. The kinetics of tumor growth was determined by measuring the volume in three perpendicular axes of the nodules using micro-scaled calipers. The efficiency of tumor formation per each tested cell was determined by the number of the mice (out of the total number of mice injected) bearing palpable tumors exceeding after 6 weeks post-injection. The palpable tumors were then harvested after sacrificing the mice. The harvest tumors were sectioned and undergone H&E staining.

## 3. RESULTS

### 3. 1 The high-throughput RNAi screening systems identified ADAM23 as a gene that is functionally associated with increased proliferative potential of HOK16B in high-serum/calcium DMEM - media

To seek out cellular changes that mediate carcinogenesis in HPV-positive HNSCC, we utilized HOK-16B, an immortalized human normal keratinocyte harboring HPV-16 genome. HOK-16B is a unique system that was developed by introduction of recombinant HPV-16 genome into Normal Human Oral Keratinocyte (NHOK). The transformed keratinocyte shows constant expression of E6 and E7 oncoproteins and continued proliferation. HOK-16B, however, does not display tumorigenic potential, as most HPV-16 infected cells do not immediately undergo malignant transformation. Hence, it is an ideal system for our investigation.

HOK-16B cells were transfected with viral RNAi Decode Library. Utilizing combined lentiviral technology and mir-shRNA, the viral RNAi particles can efficiently knock down the gene expression in host cells. There are total 7 RNAi viral pools for screening, and each pool contains about 70,000 mir-shRNAs constructs capable of knocking down the target gene individually (3-4 constructs per target gene) (Figure 1). The successfully transfected cells were initially screened using puromycin followed by culturing in DMEM based high calcium/serum media. The growth in DMEM based calcium/serum media served as another method to select the transfected cells and eliminate experimental artifact, as HOK-16B does not normally survive in this specific medium. HOK-16B pGIPZ served as a non-target control for the experiment. From the 7 viral pools used, we could isolate surviving colonies from the cells infected with lentiviral pools of 1,2, 4 and 6.

From the surviving colonies of HOK-16B, gDNA was isolated, PCR amplified and cloned into competent *E.coli* cells. Then plasmids were isolated and sequenced to identify the target genes of RNAi particles. The sequencing results showed that Pool 1 targeted SLC10A2 and Pool 2 targeted TWF-2. Furthermore, Pool 4 and Pool 6 knocked down the expression of RAB2B and ADAM23 respectively (Table 1).

### 3.2 ADAM23 expression is suppressed in HPV Positive Cancer Cell Lines

From the four target genes we identified using RNAi, we wanted to see how their expression varied in HPV positive cancer cell line. Therefore, we looked at the mRNA and protein expression of the genes in selected HPV positive cancer cell lines. We used two strains of NHOK as a control, and HOK-16B, HOK-16B/BapT, Hela, SiHa and Caski as HPV+ samples. Interestingly, we observed the ADAM23 expression was diminished in all HPV+ cancer cell lines (Figure 3A). To further differentiate the expression of ADAM23 in HPV+ cancer cells, we also looked at its expression level in HPV- cancer cells (Figure 3A). In comparison between HPV+ and HPV-HNSCCs, we clearly saw the difference in protein expression level. This differential expression of further confirmed in mRNA level using qRT-PCR (Data not shown) as well as IHC staining of HPV + cancer tissue samples (Figure 3B). This strongly suggested that ADAM23 could potentially play a role in the carcinogenesis; therefore, we decided to carry further investigation with ADAM23.

### 3.3 Knockdown of ADAM23 increased proliferative potential in high-serum/calcium medium in HPV-dependent manner

Following transfection with RNAi particles, DMEM with high calcium/serum media was used to yield final surviving HOK-16B colonies. HOK-16B cells are traditionally grown in Keratinocyte Growth Medium (KGM), and these cells do not survive in other culture medium

such as DMEM with high calcium/serum media. Growing the cells in very stringent surviving condition allowed us to further investigate altered phenotype of HOK-16B and evaluate its tumorigenic potential because for it to survive, it should be able to self-renew and continue to differentiate. We observed that these colonies not only showed survival in non-permissible DMEM media, but increased proliferation after >3 months of culture maintenance as well (Figure 4A), while the control counterpart started to senescence and ceased to proliferate. However, we weren't sure if this was solely due to knocking down of ADAM23 with Pool 4 RNAi or due to different copies of constructs in the pool affecting other gene targets. Therefore, we used independent shRNAs specific targeting three different regions of ADAM23 to attenuate the expression. Among three shRNA constructs, we saw that construct number three inhibited the ADAM23 expression the most in HOK-16B (HOK-16B/ADAM23sh-3) (Figure 5B and C). We then transferred the cells to DMEM medium and determined the rate of population doubling as before. HOK-16B/pGIPZ was used as a control. During two hundred fifty days of maintenance, two cell lines displayed markedly different course of proliferation (Figure 6A). For the first hundred days, both showed similar proliferation rate. By one hundred fiftieth day, HOK-16B/pGIPZ's rate of proliferation slowed down; by two hundredth day, all HOK-16B/pGIPZ ceased to proliferate. On the contrary, HOK-16B/ADAM23sh-3 started to show greater proliferative potential around the same time when the control group no longer survived. This result clearly showed that knocking down ADAM23 permitted HOK-16B to grow and gained greater proliferative potential in DMEM high calcium/serum medium. This implies that HOK-16B/ADAM23sh-3 acquired an ability to proliferate in environment uniquely permissive for cancer cell survival, and may suggest that the cells may acquire tumorigenic ability outside of culture media.

### 3.4 Knockdown of ADAM23 enhances tumor sphere formation and stem-cell phenotypes

Unregulated growth with accumulation of genetic mutation is one of the hallmarks in malignant transformation and development of cancer. For HPV + OSCC, this is especially important. Expression of oncoproteins E6 and E7 interaction with cell's tumor suppressor p53 and pRb respectively allows HPV infected cells to bypass the cellular regulation and continue to proliferate. As increased proliferative potential has been already demonstrated by HOK-16B/ADAM23sh-3 previously, we decided to evaluate its tumorigenic potential *in vitro*. We conducted a tumor sphere formation assay with HOK-16B/pGIPZ and HOK-16B /ADAM23i-3. The tumor sphere formation assay is widely used to identify stem cells to evaluate their self-renewal capacity and differentiation at the single cell level *in vitro*. Seven days after thousand cells of each group are seeded in non-adherent conditions with serum-free medium and epidermal growth factor supplement, the distinct tumor sphere colonies were developed by ADAM23 knocked down HOK-16B (Figure 7D). The tumor spheres formed by HOK-16B/ADAM23sh-3 were also greater in size (50-100 μm) and number compared to the pGIPZ control group (Figure 7E). This suggests that HOK-16B/ADAM23sh-3 acquired tumorigenic potential.

Following positive tumor sphere formation assay result, we decided to gain firm confirmation of this newly acquired phenotype of HOK-16B/ADAM23sh-3 using more stringent anchorage independent soft agar assay. The assay established HOK-16B/ADAM23sh-3's enhanced growth independent of solid surface as increased colony formation was observed compared its control counterpart (Figure 7F and 7G). Hence, these *in vitro* assays showed knocking-down of ADAM23 permits tumorigenicity to HOK-16B.

### 3.5 HOK16B/ADAM23sh cells cause tumor formation *in vivo*

Tumor sphere formation and anchorage independent soft agar assay demonstrated HOK-16B/ADAM23i-3's tumorigenic potential *in vitro*. To evaluate whether ADAM23 knocked down HOK-16B can develop into a tumor *in vivo*, we injected ten thousand cells subcutaneously into the flank of severely immunocompromised (nu/nu) mice (Figure 9A). Every three days, tumor development was monitored and measured. Distinct cysts started to develop after ten days post injection, and noticeable difference in its development was seen between the control groups and HOK-16B/ADAM23sh-3 by the twentieth day (Figure 9B). While cyst development ceased, and underwent senescence around thirty days post injection for the control groups, the cysts developed in HOK-16B/ADAM23i-3 mice continued until mice were harvested. However, the consistency in cyst size among the mice in this group was not observed for unknown reason.

The cysts that were collected from the mice were subjected for histological analysis using hematoxyline staining. The staining revealed active proliferation of cells inside the cyst and keratinization (Figure 9E). This indicates the injected cells were actively dividing after injection and still maintained its tumorigenic potential as observed *in vitro* assays. Therefore, HOK-16B/ADAM23i-3 demonstrated its tumorigenicity *in vitro* and *in vivo.*

### 3.6 Microarray analysis revealed differentially expressed genes in ADAM23 knocked down HOK-16B.

To further investigate the cellular changes occurred in ADAM23 knocked down HOK-16B cells, and what may contribute to its tumorigenic potential observed in the previous experiments, we ran microarray analysis to look at differential gene expression in the cells (Figure 9A). The analysis was performed in triplicate to minimize the statistical error. The analysis revealed up-regulation of various genes. Notably, SYK, CLDN-1, AQP3 and IGFB3

(Figure 9B). On the other hand, HSPA1A, KCNMA1, SCG5 and TFPI2 were significantly down-regulated in ADAM23 (Figure 9C).

### 3. 7 Inhibition of CLDN1 prevents tumorigenic potential of HOK16B/ADAM23i-3 Cells.

After confirming the differential gene expression in ADAM23 knocked genes, we decided to further investigate functional relationship between these up-regulated genes and ADAM23. Again, we have confirmed that SYK, CLDN-1, AQP3 and IGFB3 have been greatly expressed after knocking down ADAM23 with microarray analysis. To look for their functional relationship with ADAM23 and induction of tumorigenicity, we used siRNA to silence the expression of these up-regulated genes. With the genes silenced using, we performed tumor sphere formation assay. When SYK, AQP3 and IGFPB3 were silenced (Figure 12A), the tumor spheres were formed (Figure 12C). Their numbers and sizes weren't different each other (Figure 11B). When CLDN-1 expression was reduced, however, tumor forming ability of ADAM23 knocked down HOK-16B became significantly hindered. Their size and numbers were strikingly different from the other siRNA treated cells. The result of this experiment indicates a possible functional linkage between CLDN-1 and ADAM23, and contribution to the tumorigenicity of ADAM23 knocked down HOK-16B.

### 3.8 Oncoproteins E6 and E7 are necessary to increase tumorigenic potential in HOK-16B mediated by ADAM23 knockdown

Expression of oncoproteins E6 and E7, which allow the HPV infected cells to bypass regulation via their interaction with tumor suppressor p53 and pRb respectively, is important first step toward malignant transformation. Naturally, HOK-16B is a non-tumorigenic cell harboring HPV-16 genome with consistent expression of E6 and E7. However, upon knocking down ADAM23, we have seen HOK-16B gained tumorigenicity. To investigate whether E6 or/and E7

expression along with attenuation of ADAM23 is necessary for malignant transformation, we decided to target E6 or/and E7 in HOK-16B/ADAM23sh-3 using siRNA (Figure 11A and B), and repeated tumor sphere formation and soft agar assays.

Silencing E7 severely reduced the cell's ability to form tumor spheres (Figure 11D). When both E6 and E7 are silenced, the number of tumor spheres developed was significantly reduced (Figure 11C). Interestingly, when E6 was silenced alone, there was no significant attenuation in sphere formation. When these cells are subjected for the soft agar assay, silencing E6 or/and E7 significantly reduced the number of colony formation (Figure 11E and F). This suggests that knocking down ADAM23 alone does not trigger tumorigenic transformation in HOK-16B/ADAM23sh-3. The HPV oncoproteins must cooperate with ADAM23 to increase tumorigenic potential. Hence, this implies that ADAM23 plays a pivotal role in malignant transformation in HPV associated HNSCC development.

## 4. Discussion

The HPV mediated carcinogenesis starts with the viral infection affecting actively dividing keratinocytes found in oral epithelia of oral cavity and mucosal membrane in cervix. Following infection, subsequent expression of oncoproteins E6 and E7, which interact with critical tumor suppressors p53 and pRb respectively, is the first critical step leading to rise of HPV-associated malignancy. Theoretically, this would mean every HPV infection should lead to development of carcinoma. However, this is not the case. The majority of HPV infected individuals are capable of eliminating the virus using their host immune system, while only a small number of infected individuals will acquire carcinoma from the infection. This strongly proposes additional etiological factors that may favor HPV driven carcinogenesis.

Many recent studies started seeking for this additional contribution to carcinogenesis. A recent study revealed that chronic inflammation there is positive correlation in development of HPV-positive Oropharyngeal Squamous Carcinoma (OPSC) when compared to normal tissues. There was a significant increase in the rate of HPV-16 in tissues with severe chronic inflammation compared to the ones with mild and moderate inflammation[9]. Another study identified that NOTCH1 alteration accelerated tumor growth by HPV positive tumors in mice models, and additional metalloproteinase genes increased invasion, aggressive tumor growth[10].

Furthermore, high oxidation DNA damage was correlated to higher promotion of HPV carcinogenesis[11,12]. These discoveries confirm the idea HPV infection alone is not enough to develop carcinoma.

The aim of this study was to discover this additional perturbation that leads to HPV-mediated carcinogenesis by introducing a cellular alteration using a novel high-throughput

Decode RNAi Screening Library. Cellular changes induced by RNAi particles will be detected using stringent selection criteria, and identified using unique method of identification.

Following transfection with the viral pools, we were able to detect alterations induced by RNAi particles. We discovered expression of four genes was four target genes were attenuated, which conferred resistance and growth in DMEM high calcium/media. The four identified target genes are SLC10A2, TWF2, RAB2B and ADAM23.

SLC10A2 is a sodium/bile acid transporter that is involved in bile acid transportation from the large intestine and cholesterol homeostasis[13]. Its mutation has been reported to be associated with liver and intestinal diseases[14]. TWF2 encodes a protein containing an actin and ATP-binding site[15]. RAB2B is a membrane bound protein playing a role in vesicular fusion and trafficking[16]. While these genes have important physiological implications, they showed no significant relevance to cancer development. However, ADAM23, a putative tumor suppressor, has been consistently implicated in different cancer cases such as gastric and breast cancer to be silenced. In addition, protein analysis of selected HPV positive OPSCs revealed reduction in ADAM23 expression as well as in mRNA level. Therefore, we decided to investigate ADAM 23's functional role in HPV driven carcinogenesis.

ADAM23, A Disintegrin And Metalloproteinase 23, is a membrane bound protein with structural similarity to snake venome disintegrins. ADAM23 has been implicated in many biological processes such as cell-cell and cell-matrix interactions[17] such as fertilization, muscle development, and neurogenesis[18]. Its inactivation leads to tumorigenesis in human cancer; however, its mechanism that leading to carcinogenesis is unclear. ADAM23 is frequently studied in the context of neurogenesis along with its family member protein ADAM22. Both members of

ADAM family proteins contain disintegrin domain where Leucine-rich, glioma activated (LGI1) neuronal protein binds to presynaptic ADAM23 and postsynaptic ADAM22 proteins[19]. Silencing of ADAM23 has been heavily implied in the development of epilepsy during development[19]. In fact, multiple animal studies have demonstrated that ADAM23 knockout mice suffer from frequent seizures and difficulties in suckling not permitting the mice to survive beyond the early postnatal period[19,20]. ADAM23 is widely expressed mainly in the pyramidal cells of the cerebral cortex as well as some regions of the hippocampus of the Central Nervous System[19].

In the context of carcinogenesis, ADAM23 is frequently silenced in gliomas, breast, pancreatic, gastric, head and neck, colorectal and even lung tumors[21]. The studies have shown that ADAM23's promoter region was hypermethylated in the lung and colorectal cancer cell lines[17,22]. When ADAM23 is knocked out a cell shows increased invasion, enhanced migration and cell adherence [21]. It is believed that ADAM23 negatively modulate $\alpha_v\beta_3$ integrin activation as higher metastatic breast cancer frequently showed higher degree of promoter methylation, hence, ADAM23 silenced[23]. In intratumoral heterogeneity population of ADAM23 negative and positive cancerous cells, it has been shown that ADAM23 negative cells promoted tumor growth and metastasis of ADAM23 positive via cell-to-cell communication via LGI4[21]. Considering cancerous tissue rises from heterogeneous population of cancer cells, this indicates knocking down of ADAM23 in a malignant cell greatly enhances its tumorigenic potential. However, via what mechanism ADAM23 enhances cancerous phenotype is still unclear. Furthermore, this is the first study investigating the functional role of ADAM23 in HPV mediated carcinogenesis.

Consistent with previous findings, knocking down of ADAM23 from HOK-16B vastly improved proliferative potential of the cells. It was surprising to see HOK-16B was able to grow in the medium, which doesn't normally permit HOK-16B to proliferate. When usually HOK-16B

is cultured in DMEM medium, it will last only a few passages before it starts to senescence and cease to proliferate. However, with ADAM23 knocked down, HOK-16B continued to proliferate. Given that there is consistent expression of E6 and E7 present in HOK-16B, but cannot proliferate in DMEM, its ability to proliferate in DMEM can solely be attributed to knocking down ADAM23 as compared to wildtype HOK-16B grown in DMEM. We also utilized three separate constructs of ADAM23 shRNAs targeting different regions in the coding sequence, and we saw the same phenotype as previously.

The difference in proliferative potential between HOK-16B/pGIPZ and HOK-16B/ADAM23sh was observed after >3 months. We are unclear why it took >3 months for the difference to occur. A possible explanation for this difference could be that silencing of ADAM23 and cellular alteration requires some time to take effect. In fact, we have tested to see if tumorigenic potential increased immediately after using shRNA by performing tumor sphere formation assay. However, we could not obtain the tumor spheres when the assay was performed (Data not shown). This further confirms the stable alteration takes some time for the alteration to become stable, and its phonotypical change starts to manifest after >3 months. It is something we could further look in the future study investigating unidentified subsequent alterations.

Tumor sphere formation assay is useful in evaluating self-renewal capacity and differentiation of a single stem cell. This has been widely used in cell and cancer biology. A positive test result from this classic assay indicates that HOK-16B has undergone transformation and obtained cancer stem cell like characteristics. It has been noted that HPV infection and subsequent expression of oncoproteins E6 and E7 are the hallmark of carcinogenesis in many HPV positive cancers. Many studies also looked into the effects of E6 and E7 on cancer stemness. Looking at the cancer stem cell population in HPV positive head and neck SCC has

shown that E6 tends to increase the stemness as it helps the cell evade p53 regulation which resulted tumor formation *in vivo* involving SCID mice. Another study could demonstrate that transduction of E6/E7 into the HPV-negative cancer cell to increase colony formation and resistance to Cisplatin, a characteristic of HNSCC CSC. However, when tail vein injected into mice, there was no difference in lung colony formation. These studies point out that E6 and E7 are important for developing and maintaining CSC in HNSCC. However, CSC needs to be maintained and allow cells to continue to renew itself is a requirement for tumor formation. E6 and E7 may increase the CSC for some period, however, it may not maintain its phenotype of a prolonged period of time. This further indicates that additional cellular alteration or genetic event needs to take place to maintain cancer stemness. According to our study, we believe silencing of ADAM23 is the additional genetic event that helps E6 and E7 to maintain CSC characteristics. Other studies have indicated that ADAM23 negative cancer cell showed greater proliferation and metastasis. In heterogeneous population of gastric cancer cells, where there are ADAM23 negative and ADAM23 positive cells, ADAM23 negative cells secrete LGI4, and allow ADAM23 positive cells to undergo rapid proliferation and metastasis. Since we used HOK-16B as our model and used shRNA technology to silence ADAM23 expression, we did not have heterogeneous population. However, the phonotypical change that took place with ADAM23 silencing coincided with our study. Increased CSC characteristic was further confirmed in the anchorage independent soft agar assay. The soft agar assay considered to be the most stringent assay for detecting malignant transformation of cells as the ability for cells to grow independently of a solid surface is a hallmark of carcinogenesis. Because HOK-16B/ADAM23 formed colonies in this assay, we confirmed its malignant transformation, and this was further supported in our *in vivo* assay with immunocompromised nude mice. In summary, silencing of

ADAM23 triggered HOK-16B to gain cancer stem cell characteristics and undergo malignant transformation allowing the cells to gain tumorigenicity *in vitro* and *in vivo*.

The one of the greatest challenges in our investigation was that the function of ADAM23 has not been well documented. ADAM23 has been suggested as a tumor suppressor in many cancer studies as its expression diminished in the cancer cells or tissues, however, the information about how it regulates tumorigenic potential of cell or cellular pathway association is very scarce now. To better understand this, we decided to conduct microarray analysis of genome of HOK-16B/ADAM23 to see what genes became upregulated or downregulated. A wide array of genes was prominently upregulated in ADAM23 knocked down HOK-16B. Among the genes that showed increase in expression, we decided to further investigate CLDN-1. CLDN-1 is a protein found in the tight junctions of cells. It essentially helps anchoring the cells together and come in close contact with one another. Therefore, high expression of CLDN-1 may create an environment that may enhance tumor formation as the cells are in close contact with another. CLDN-1 may explain the reason why HOK-16B/ADAM23 exhibited increased tumorigenicity. Increased expression of CLDN-1 is frequently found in aggressive breast cancer cases. High expression of this gene led to increased migration and metastasis while suppressing CLDN-1 reduced cell proliferation, survival and invasion. Furthermore, it has also inhibited epithelial to mesenchymal transition state. In our study, we also silenced CLDN-1 using siRNA, and confirmed significant decrease in tumorigenic potential as observed in the tumor sphere formation assay. Less tumor spheres were formed after silencing CLDN-1 expression. This coincides with the phenotype of CLDN-1 silenced; therefore, we can establish that high expression of CLDN-1 could also culminate to malignant transformation following ADAM23 knock down and HPV oncoprotein expression. Furthermore, high expression of CLDN-1

following ADAM23 silencing may indicate that ADAM23 may exert negative feedback on CLDN-1 expression. However, it is the relationship is unclear.

To determine how ADAM23 is functionally related to E6 and E7, we decided to use siRNAs to knock down E6 or/and E7 expression. With E6 and E7 silenced, we believed that tumor sphere formation would be stunted even with ADAM23 silenced as E6 and E7 play a pinnacle role in carcinogenesis. Interestingly, we have seen that knocking down of E7 affected the tumor formation more than E6, while silencing both E6 and E7 had severe effects on the cells ability to form sphere. This may indicate E7 may play a greater role in increasing tumorigenic potential than E6 as pRb is more directly related to the progression of cell cycle. While E6 interaction with p53 is an important event for development of malignancy and evading apoptosis of the cell, however, based on our result, it suggests that E6 alone is not enough to trigger the transformation. This further supports our hypothesis that additional genetic event must take place for cancerous development. With E6 and E7 silenced, there was decreased tumorigenic potential in HOK-16B/ADAM23. This indicates that silence of ADAM23 is not enough for malignant transformation. It must be that E6, E7 and ADAM23, cooperate to yield malignancy. This supports that silencing of ADAM23 is indeed the additional genetic alteration that needs to take place for carcinogenesis.

In conclusion, this study provides novel information about HPV-positive HNSCC. It was believed that E6 and E7 expression following HPV infection is a hallmark of HPV-mediated carcinogenesis. However, we believed that there is additional factor that drives the malignant transformation. Utilizing high-throughput screening method, we have identified ADAM23 as a potential genetic event that contribute to carcinogenesis. We have shown that silencing of ADAM23 does indeed grant tumorigenic potential to non-tumorigenic HOK-16B. We were also

able to confirm that ADAM23 may have cooperative relations with E6 and E7 in carcinogenesis. The next task in this investigation is to look how they are working together. With that knowledge, we would be able to evaluate ADAM23 as a useful prognostic marker for screening individuals with high risk of developing HPV-positive HNSCC.

## Figure Legends and Figures

### Figure 1: Schematic representation of RNAi Decode Library and flow chart.

Each pool contains about 10,000 shRNAmir construct with 3 to 4 variations. After the target has been successfully knocked -down, a specific set of primers flanking the construct could be used to identify the targeted gene by RNAi particle. Following RNAi transfection, initial surviving colony was obtained by Puromycin resistance, and then grown in DMEM/FBS medium to yield final surviving colony. Then gDNA was collected and sequenced to identify the targets of RNAi particles.

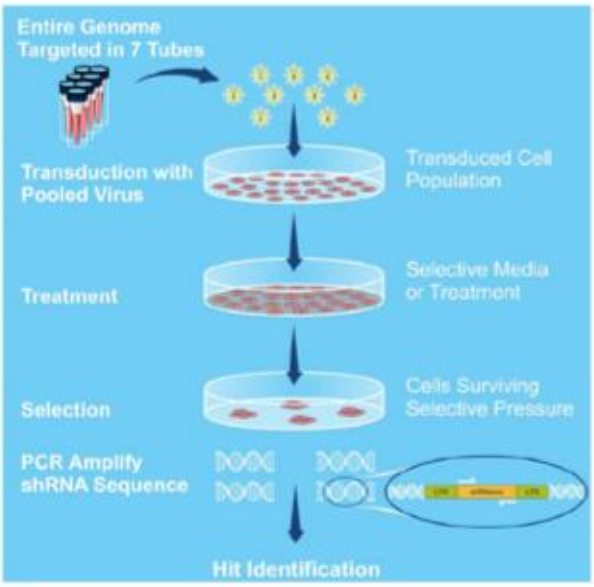


7 vials of lentiviral pools (10,000 shRNAmir constructs)
3-4 constructs per gene
Can use specific primers to identify shRNA sequences
Identify the target genes

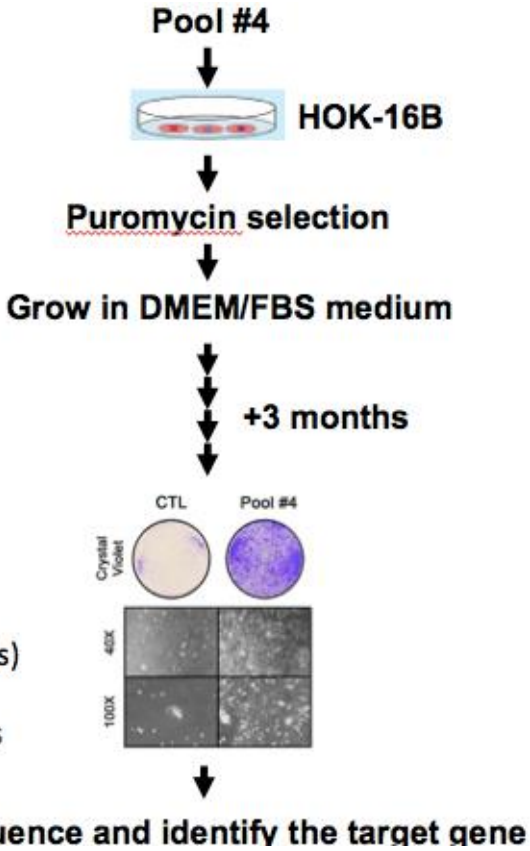

**Figure 2: Phase Contrast and Green Fluorescence Microscopy of HOK-16B following transfection with RNAi pools.**

Left panels show phase contrast images of HOK-16B and right panels show green fluorescence images HOK16B after transfection with RNAi pools.

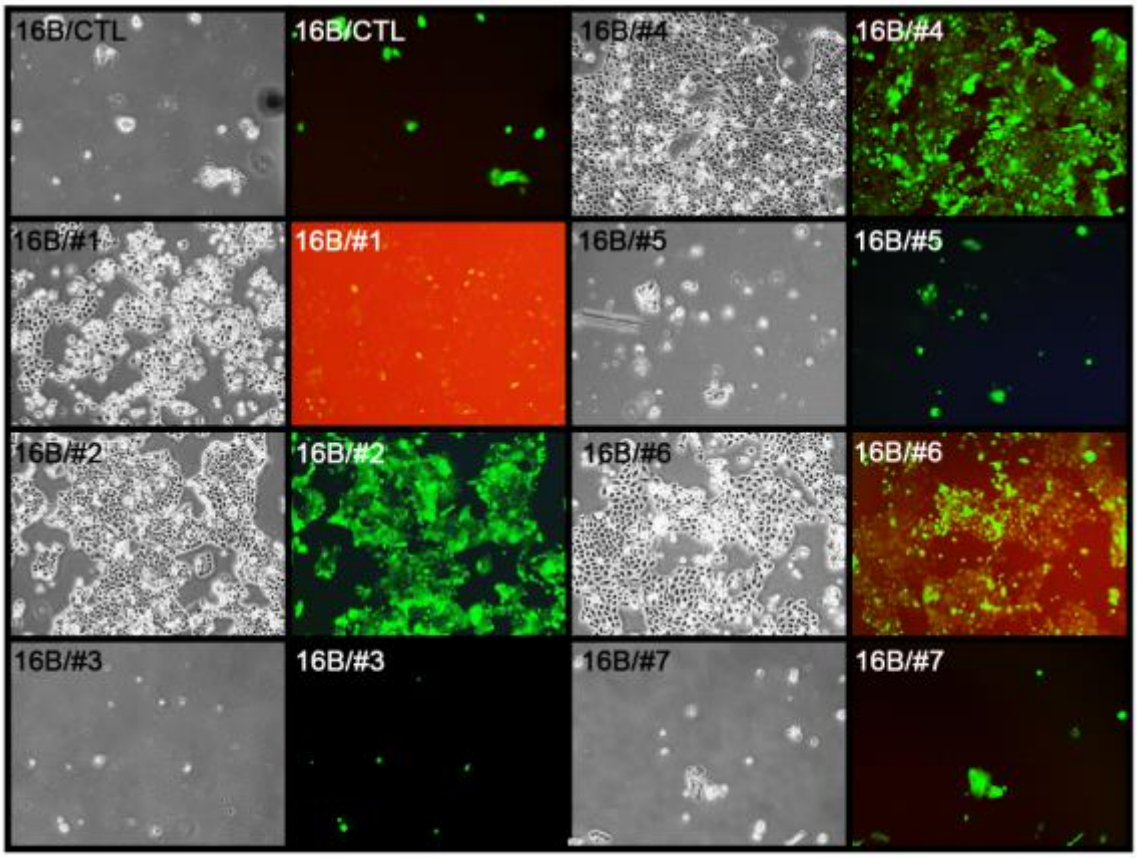
16B/CTL
16B/CTL
16B/#4
16B/#4
16B/#1
16B/#1
16B/#5
16B/#5
16B/#2
16B/#2
16B/#6
16B/#6
16B/#3
16B/#3
16B/#7
16B/#7

**Table 1: Genes identified from the high-throughput RNAi Screening System**

After the transfection with RNAi particles, the cells were initially selected with puromoycin resistance. Following anti-biotic resistance, the cells were selected against stringent growth condition (DMEM + 10% FBS) to yield final surviving colonies. Then the surviving colonies were then collected and gDNA isolated. Following the manufacturer's protocol, RNAi target genes were identified.

Table 1: Genes identified from the high-throughput screening system

| | Chro. | Gene name | Oligo ID (Open Biosystems) | Gene ID (Pub Med) | Functions |
|---|---|---|---|---|---|
| shRNA pool #1 | 15q25<br>13q33 | Unknown<br>SLC10A2 | 265749<br>270936 | -<br>6555 | Unknown<br>Sodium/bile acid transporter |
| shRNA pool #2 | 6p12<br>3q21.1 | Unknown<br>TWF2 | 102785<br>91138 | -<br>11344 | Unknown<br>Twinfilin, actin-binding protein, homolog 2 |
| shRNA pool #4 | 13q12<br>14q11.2 | Unknown<br>RAB2B | 74299<br>177837 | -<br>84932 | Unknown<br>RAB2B, member RAS oncogene family |
| shRNA pool #6 | 2q33 | ADAM23 | 241170 | 8745 | A disintegrin and metalloprotease domain |

**Figure 3. ADAM23 expression is significantly suppressed in HPV- positive OSCCs.**

A) Western blotting analysis evaluating protein levels of identified genes from RNAi screening in selected HPV positive and negative OSCC samples. ADAM23 expression significantly reduced in HPV + OSCCs. B) Immunohistochemical staining of OSCC tissue representing expression of ADAM23. The tissues show attenuated expression of ADAM23 in the tissues.

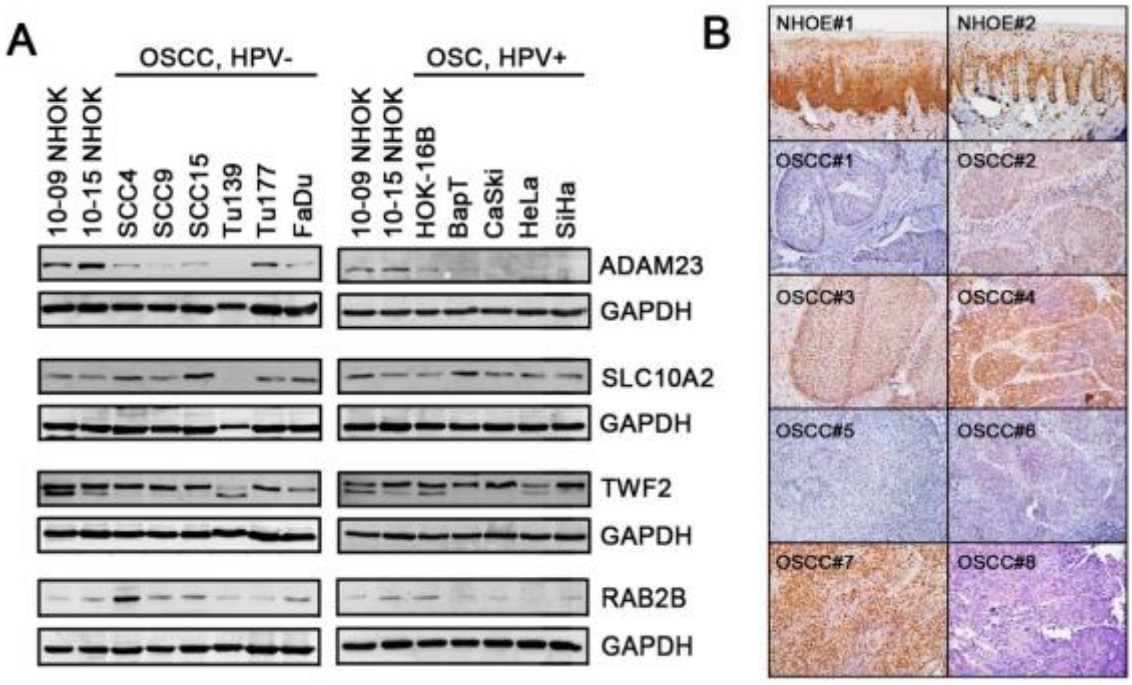
A
OSCC, HPV-
OSC, HPV+
10-09 NHOK
10-15 NHOK
SCC4
SCC9
SCC15
Tu139
Tu177
FaDu
10-09 NHOK
10-15 NHOK
HOK-16B
BapT
CaSki
HeLa
SiHa
ADAM23
GAPDH
SLC10A2
GAPDH
TWF2
GAPDH
RAB2B
GAPDH
B
NHOE#1
NHOE#2
OSCC#1
OSCC#2
OSCC#3
OSCC#4
OSCC#5
OSCC#6
OSCC#7
OSCC#8

**Figure 4. Knocking down of ADAM23 from HOK-16B increases the cells proliferative potential.**

A) Relative ADAM23 mRNA level difference after transfection with RNAi particles. B) Cell proliferation curves depicting the rate of population doublings between HOK-16B transfected with CTLsh, and ADAM23sh. The cells were maintained for >3 months. C) Crystal violet staining indicating difference in the proliferative potential between CTLsh and ADAM23sh. D) Phase contrast and green fluorescence microscopy of CTLsh and ADAM23.

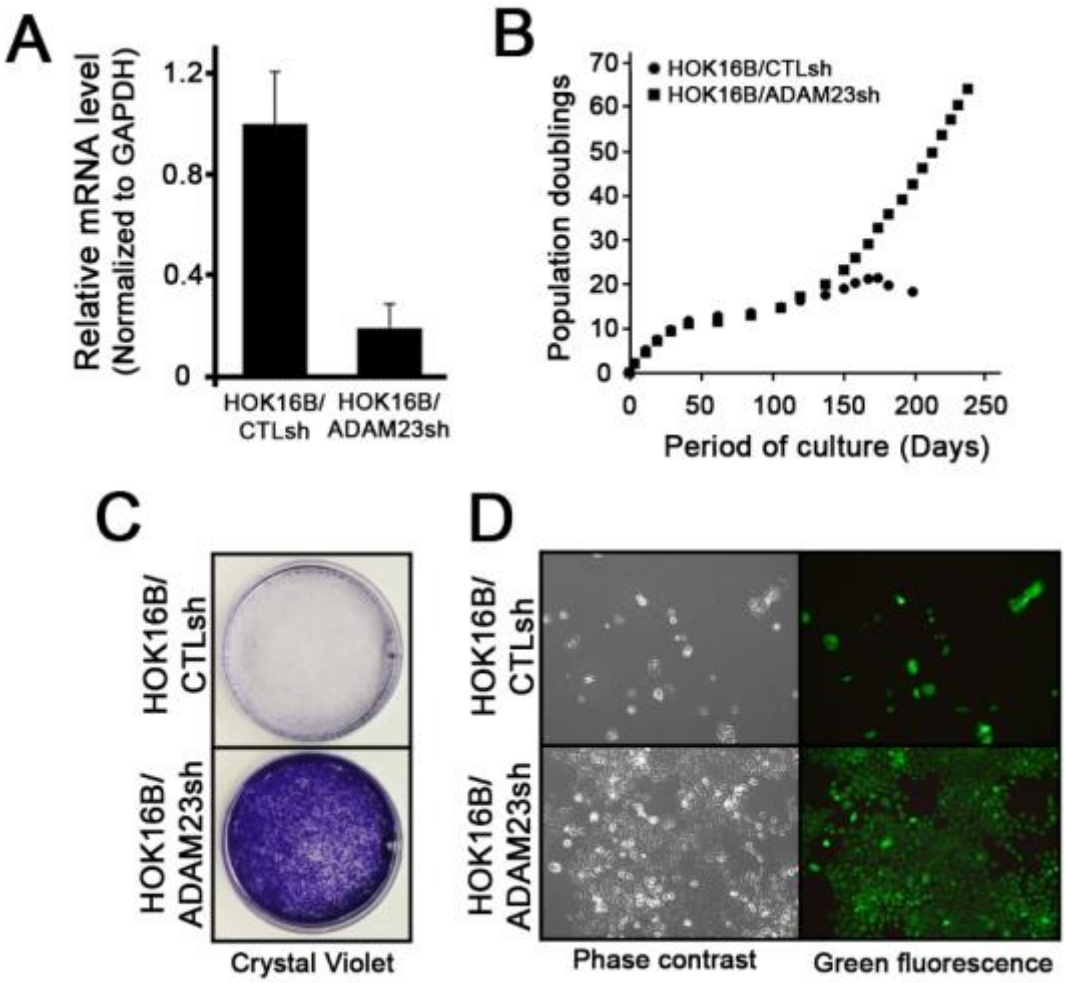
A
Relative mRNA level
(Normalized to GAPDH)
1.2
0.8
0.4
0
HOK16B/
CTLsh
HOK16B/
ADAM23sh
B
HOK16B/CTLsh
HOK16B/ADAM23sh
Population doublings
70
60
50
40
30
20
10
0
0
50
100
150
200
250
Period of culture (Days)
C
HOK16B/
CTLsh
HOK16B/
ADAM23sh
Crystal Violet
D
HOK16B/
CTLsh
HOK16B/
ADAM23sh
Phase contrast
Green fluorescence

**Figure 5. shRNA Construct #3 of ADAM23 Showed Greatest Attenuation of ADAM23 Expression in HOK-16B.**

Three different constructs of ADAM23 shRNA targeting different coding regions of ADAM23. ADAM23sh-1 targets the 5' end of ADAM23 CDS, and ADAM23sh-2 and -3 target toward the 3' end of ADAM23 CDS. A) Phase contrast and green fluorescence microscopy showing transfection efficiency of three copies of shRNAs used. B) Quantification of mRNA level of ADAM23 in HOK-16B indicates construct copy #3 most effectively knocked down ADAM23. C) Western blot analysis confirms shRNA #3 most effectively knocked-down ADAM23 level in HOK-16B.

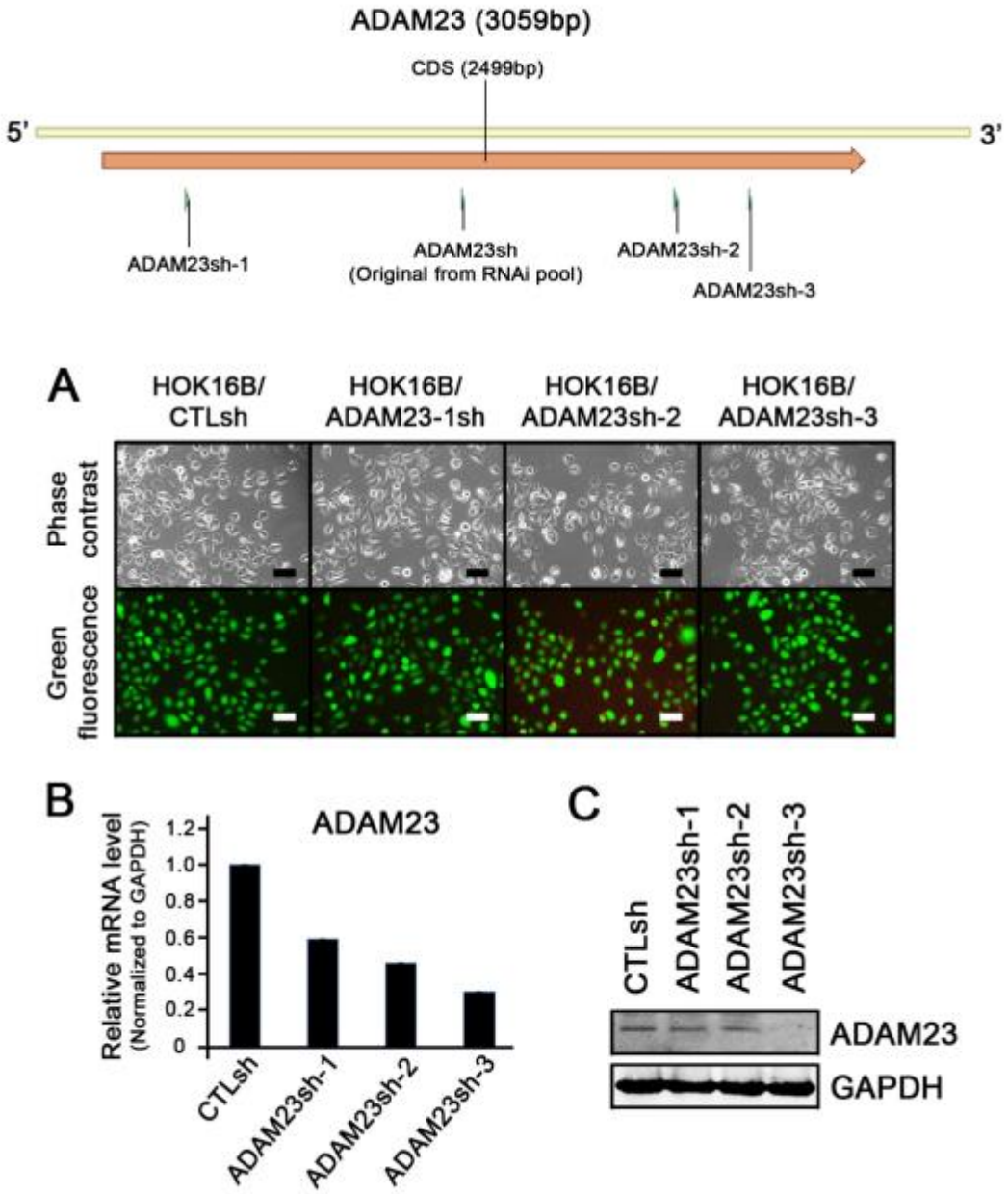
ADAM23 (3059bp)
CDS (2499bp)
5'
3'
ADAM23sh-1
ADAM23sh
(Original from RNAi pool)
ADAM23sh-2
ADAM23sh-3
A
HOK16B/
CTLsh
HOK16B/
ADAM23-1sh
HOK16B/
ADAM23sh-2
HOK16B/
ADAM23sh-3
Phase contrast
Green fluorescence
B
ADAM23
Relative mRNA level
(Normalized to GAPDH)
1.2
1.0
0.8
0.6
0.4
0.2
0
CTLsh
ADAM23sh-1
ADAM23sh-2
ADAM23sh-3
C
CTLsh
ADAM23sh-1
ADAM23sh-2
ADAM23sh-3
ADAM23
GAPDH

**Figure 6: Increased proliferative potential after knocking-down ADAM23 was confirmed in a repeated cell proliferation monitoring.**

A) Population doubling after ADAM23sh-3 used to knock down ADAM23 expression in HOOK-16B.Same proliferation pattern was observed as previously. B) Phase contrast and green fluorescence microscopy after transfecting with ADAM23sh-3 RNAi.

A.

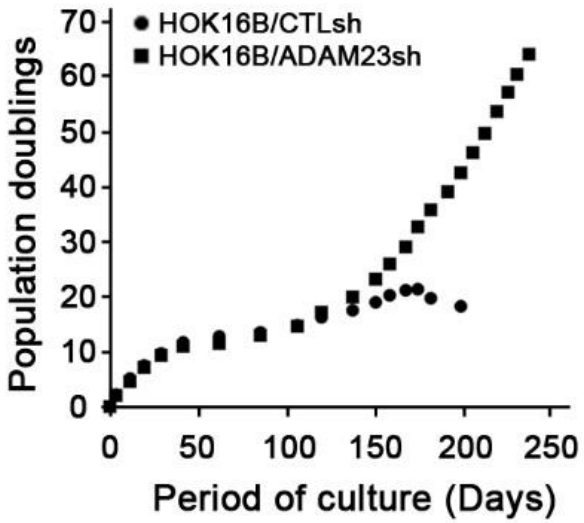
HOK16B/CTLsh
HOK16B/ADAM23sh
Population doublings
70
60
50
40
30
20
10
0
0
50
100
150
200
250
Period of culture (Days)

B.

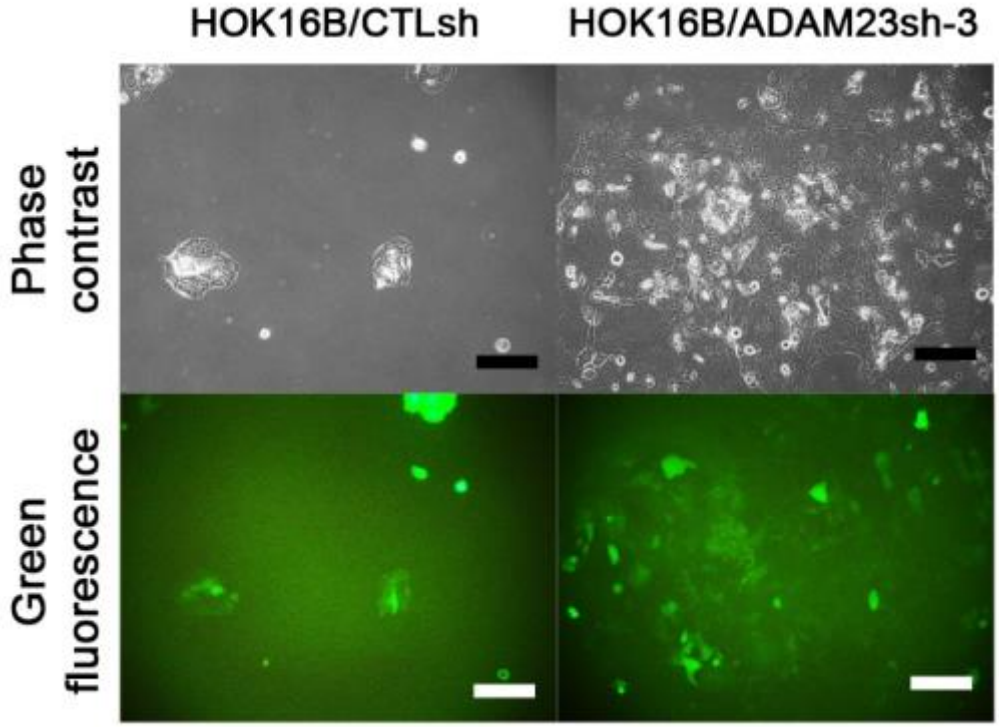
HOK16B/CTLsh
HOK16B/ADAM23sh-3
Phase contrast
Green fluorescence

**Figure 7. Knocking down ADAM23 expression increased tumorigenic potential in *in vitro* sphere formation assay and anchorage independent soft agar assay**

D) Development of tumor spheres from three different groups of cell lines. HOK-16B/CTLsh, HOK-16B/ADAM23sh and SCC4 (negative control) after 1000 cells were plated and incubated for 5 days. E) Difference in sphere numbers relative their sizes. SCC4 showed development of greatest number of tumor spheres and greater in size. ADAM23sh showed second greatest development of tumor sphere and size. F) Anchorage independent soft agar assay colony formation assay confirmed increased tumorigenic potential by HOK-16B/ADAM23sh. G) Number of surviving colony formation following anchorage independent soft agar assay by the cell lines.

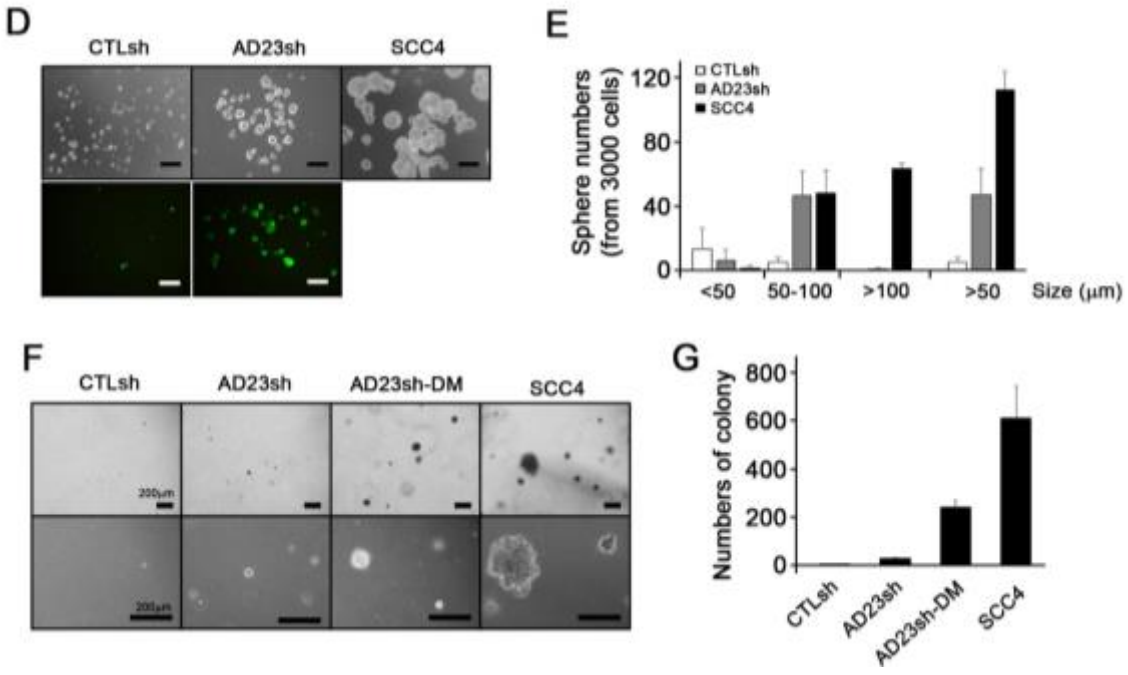
D
CTLsh
AD23sh
SCC4
E
CTLsh
AD23sh
SCC4
Sphere numbers (from 3000 cells)
120
80
40
0
<50
50-100
>100
>50
Size (μm)
F
CTLsh
AD23sh
AD23sh-DM
SCC4
200μm
200μm
G
Numbers of colony
800
600
400
200
0
CTLsh
AD23sh
AD23sh-DM
SCC4

**Figure 8. Organotypic RAFT Culture**

Oragnotypic RAFT culture assay shows tissue differentiation in normal HOK16B, however, there is no differentiation shown in HOK16B/ADAM23i.

HOK16B/
GIPZ
HOK16B/
ADAM23i

**Figure 9. Knocking down of ADAM23 from HOK-16B increases tumorigenic potential *in vivo*.**

A) mice with tumor development following injection of 10,000 cells of HOK-16B/CTLsh, HOK-16B/ADAM23(KGM) and HOK-16B/ADAM23 (DMEM). 5 mice were used per group and total of 15 mice. B) Tumor growth was closely monitored for fifty days, and ADAM23sh/DM showed greatest growth in size. C) Physical representation of harvested tumors fifty days post injection. D) Weight difference between the harvest tumors. E) Harvested tumors were sectioned and subjected for H&E staining. Black square indicates cell proliferation and keratinization inside the developing tumors.

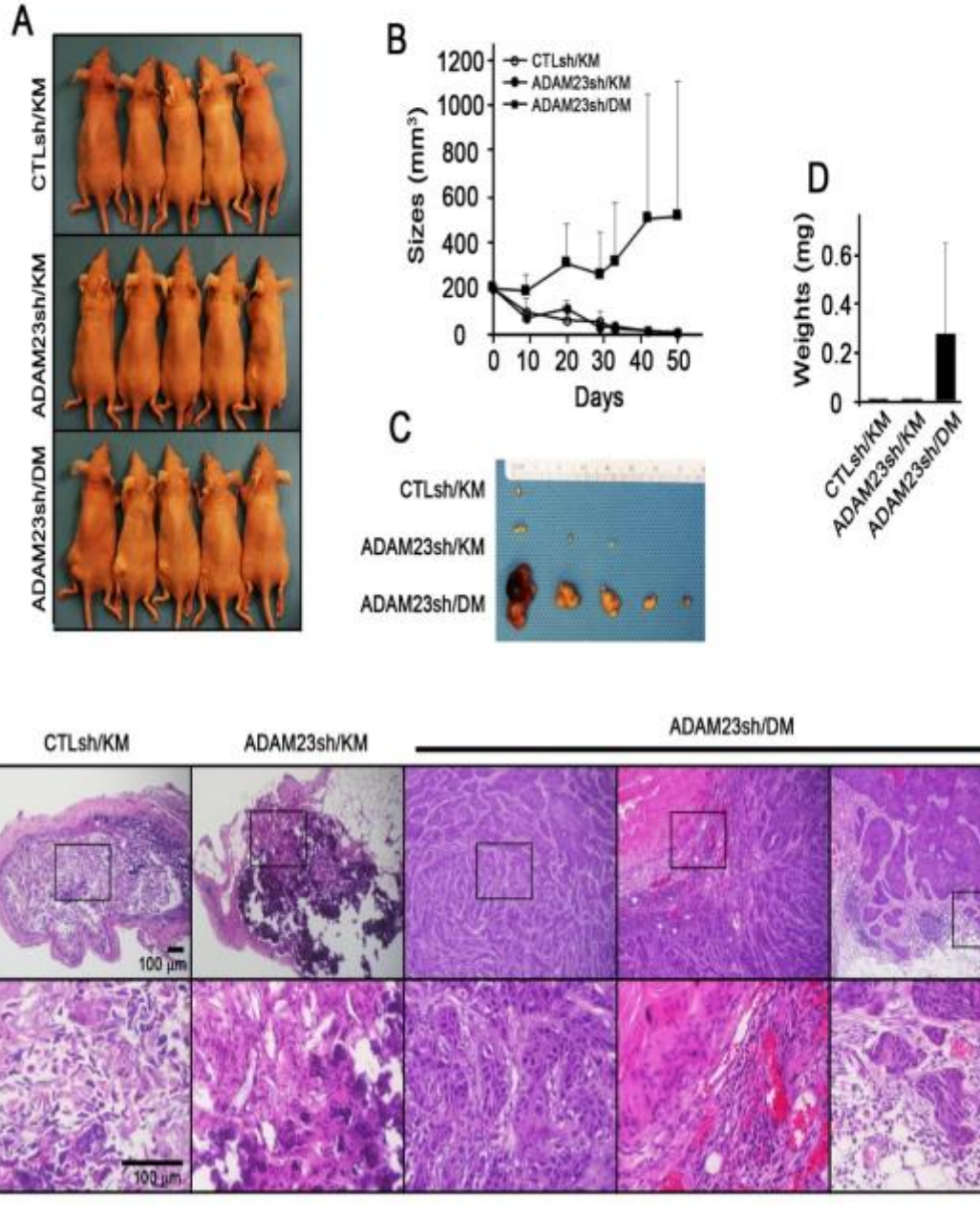
A
CTLsh/KM
ADAM23sh/KM
ADAM23sh/DM
B
CTLsh/KM
ADAM23sh/KM
ADAM23sh/DM
Sizes (mm³)
1200
1000
800
600
400
200
0
0 10 20 30 40 50
Days
C
CTLsh/KM
ADAM23sh/KM
ADAM23sh/DM
D
Weights (mg)
0.6
0.4
0.2
0
CTLsh/KM
ADAM23sh/KM
ADAM23sh/DM
E
CTLsh/KM
ADAM23sh/KM
ADAM23sh/DM
100 μm
100 μm

**Figure 10. Microarray analysis depicting differential expression of genes after knocking down ADAM23 from HOK-16B.**

A) Heat map displaying differential expression of genes after knocking down ADAM23 from HOK-16B. B) Confirmation of up-regulated genes (CCNA1, SMAD9, PCDH7, SYK, BTBD11, CLDN1, S100A8, PI3, S100A9, AQP3, IGFB3) following microarray analysis via qRT-PCR. C) Confirmation of down-regulated genes (ETV5, GRAMD1C, HSPA12A, KCNMA1, SCG5, TFPI2, CDH11, PLD5, FN1) following microarray analysis via qRT-PCR.

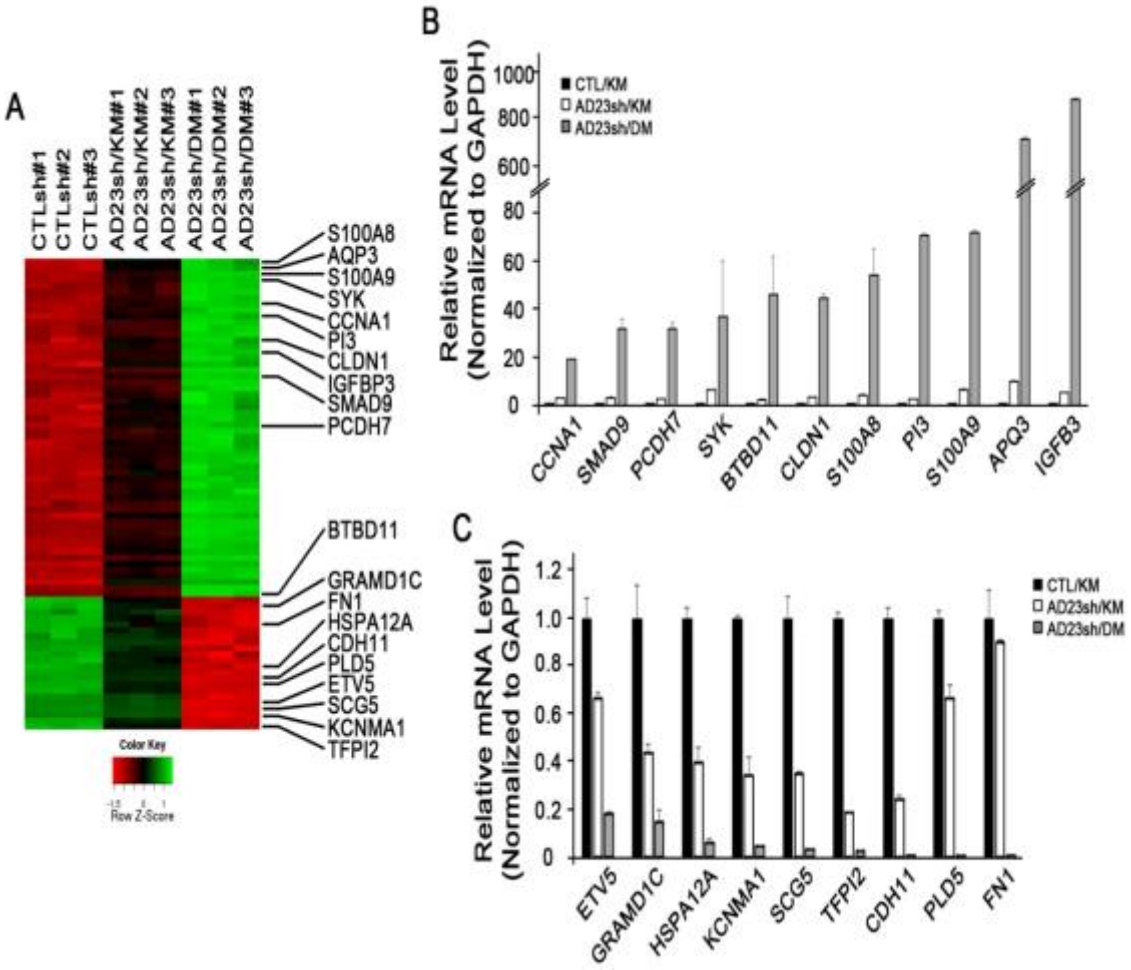
A
CTLsh#1
CTLsh#2
CTLsh#3
AD23sh/KM#1
AD23sh/KM#2
AD23sh/KM#3
AD23sh/DM#1
AD23sh/DM#2
AD23sh/DM#3
S100A8
AQP3
S100A9
SYK
CCNA1
PI3
CLDN1
IGFBP3
SMAD9
PCDH7
BTBD11
GRAMD1C
FN1
HSPA12A
CDH11
PLD5
ETV5
SCG5
KCNMA1
TFPI2
Color Key
Row Z-Score
B
Relative mRNA Level
(Normalized to GAPDH)
CTL/KM
AD23sh/KM
AD23sh/DM
CCNA1
SMAD9
PCDH7
SYK
BTBD11
CLDN1
S100A8
PI3
S100A9
APQ3
IGFB3
C
Relative mRNA Level
(Normalized to GAPDH)
CTL/KM
AD23sh/KM
AD23sh/DM
ETV5
GRAMD1C
HSPA12A
KCNMA1
SCG5
TFPI2
CDH11
PLD5
FN1

**Figure 11. Knocking-down ADAM23 increases tumorigenic potential cooperatively with oncoproteins E6 and E7.**

ADAM23 knocked-down cells consistent expression of E6 and E7. A and B) siRNA specifically targeting E6 and E7 expression in HOK-16B/ADAM23 was used to attenuate their expression. C) Development of tumor spheres in tumor sphere formation assay following E6 or/andE7 knock- down with siRNAs. D) Development of colony formation in anchorage independent soft agar assay following E6 or/and E7 knock-down with siRNAs.

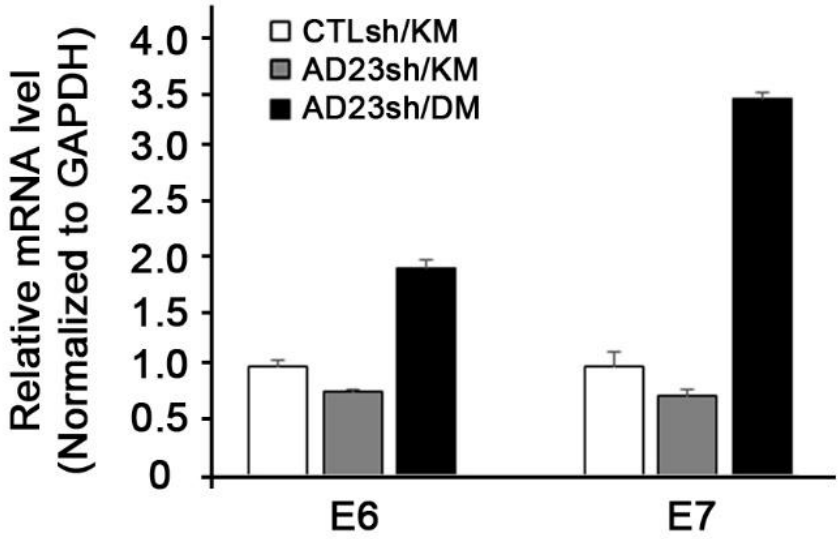
Relative mRNA lvel
(Normalized to GAPDH)
4.0
3.5
3.0
2.5
2.0
1.5
1.0
0.5
0
CTLsh/KM
AD23sh/KM
AD23sh/DM
E6
E7

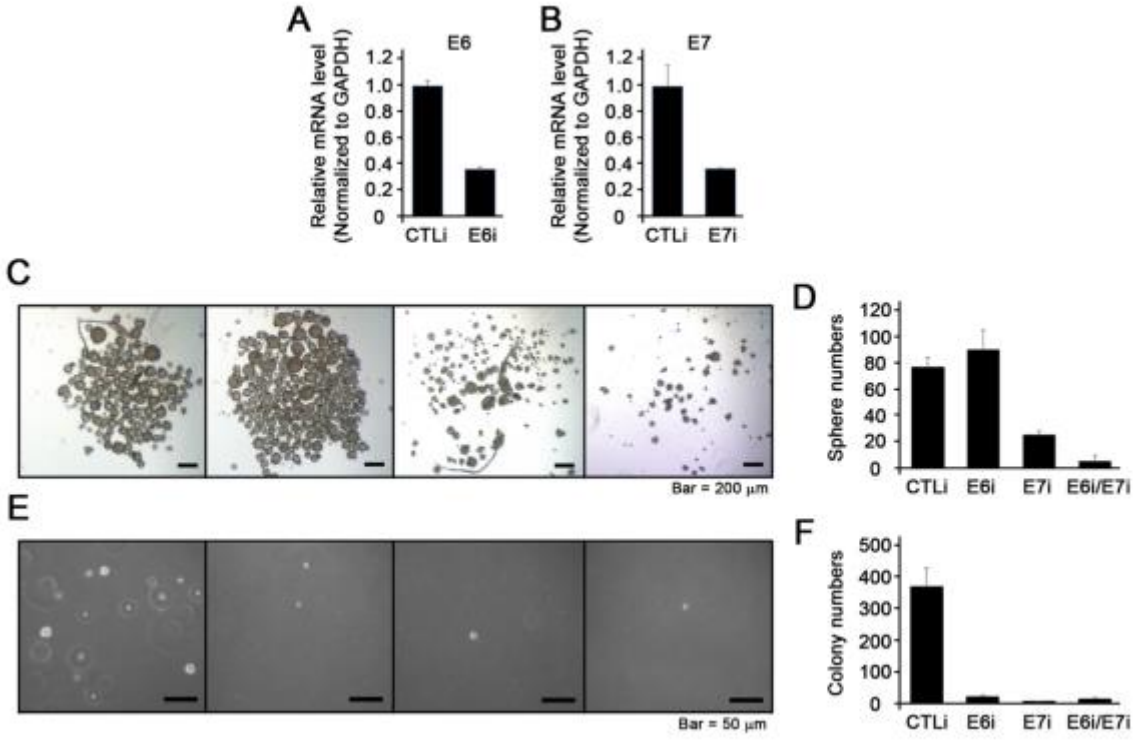
A
Relative mRNA level
(Normalized to GAPDH)
E6
1.2
1.0
0.8
0.6
0.4
0.2
0
CTLi
E6i
B
Relative mRNA level
(Normalized to GAPDH)
E7
1.2
1.0
0.8
0.6
0.4
0.2
0
CTLi
E7i
C
Bar = 200 μm
D
Sphere numbers
120
100
80
60
40
20
0
CTLi
E6i
E7i
E6i/E7i
E
Bar = 50 μm
F
Colony numbers
500
400
300
200
100
0
CTLi
E6i
E7i
E6i/E7i

**Figure 12. Silencing CLND-1 expression with siRNA decreases tumorigenic potential in HOK-16B/ADAM23i-3.**

A) mRNA expression of SYK, IGFPB3, AQP3 and CLDN-1 following transfection with siRNA. B) Number of sphere formation by the cells after siRNA treatment. C) Difference in tumor sphere formation by the cells following siRNA treatment. The assay was conducted for total 5 days.

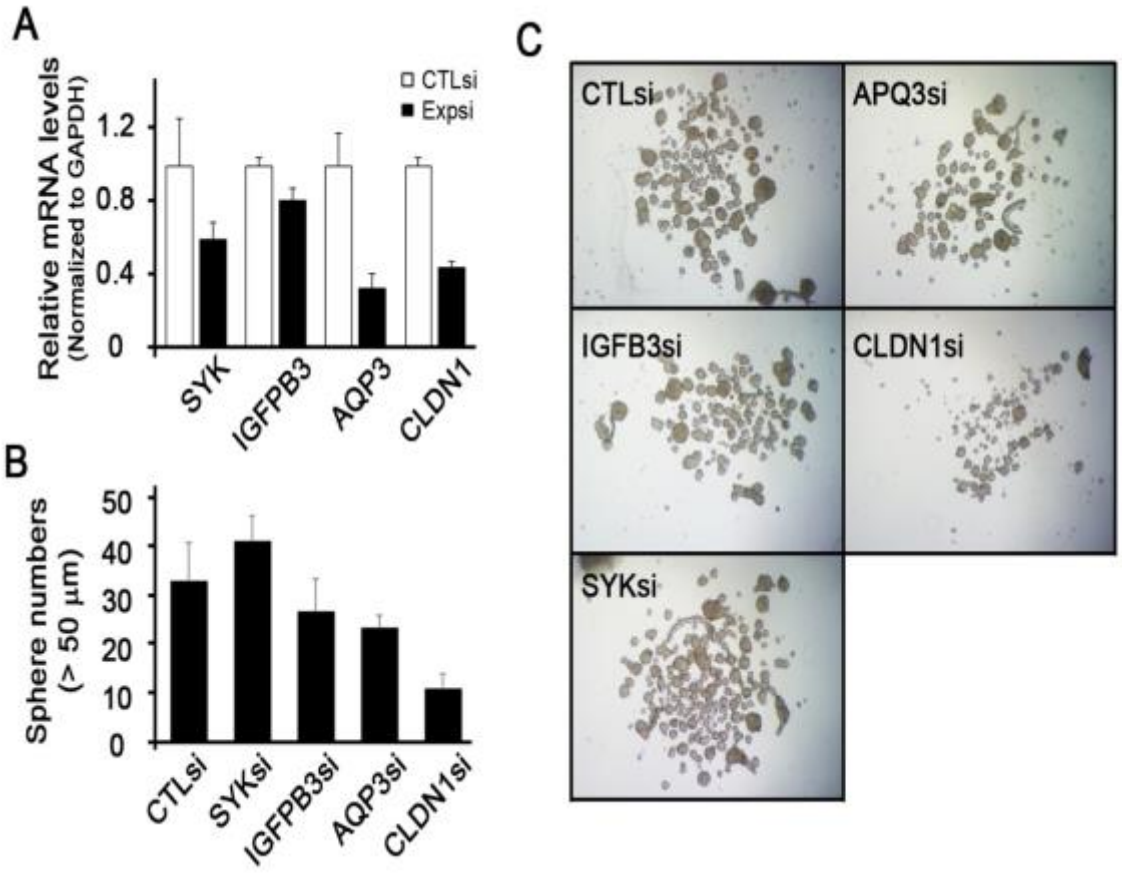
A
Relative mRNA levels
(Normalized to GAPDH)
CTLsi
Expsi
1.2
0.8
0.4
0
SYK
IGFPB3
AQP3
CLDN1
B
Sphere numbers
(> 50 µm)
50
40
30
20
10
0
CTLsi
SYKsi
IGFPB3si
AQP3si
CLDN1si
C
CTLsi
APQ3si
IGFB3si
CLDN1si
SYKsi

## References


1. Hausen, H.z. <Papillomvirus infections - a major cuase of human cancers.pdf>. (1996).

2. Scheurer, M.E., Tortolero-Luna, G. & Adler-Storthz, K. Human papillomavirus infection: biology, epidemiology, and prevention. *Int J Gynecol Cancer* **15**, 727-746 (2005).

3. Hellner, K. & Munger, K. Human papillomaviruses as therapeutic targets in human cancer. *J Clin Oncol* **29**, 1785-1794 (2011).

4. Panwar, A., Batra, R., Lydiatt, W.M. & Ganti, A.K. Human papilloma virus positive oropharyngeal squamous cell carcinoma: a growing epidemic. *Cancer Treat Rev* **40**, 215-219 (2014).

5. Chaturvedi, A.K., *et al.* Human papillomavirus and rising oropharyngeal cancer incidence in the United States. *J Clin Oncol* **29**, 4294-4301 (2011).

6. Gillison, M.L., *et al.* Distinct risk factor profiles for human papillomavirus type 16-positive and human papillomavirus type 16-negative head and neck cancers. *J Natl Cancer Inst* **100**, 407-420 (2008).

7. de Witte, C.J., *et al.* Imiquimod in cervical, vaginal and vulvar intraepithelial neoplasia: A review. *Gynecol Oncol* (2015).

8. Dongari-Bagtzoglou, A. & Kashleva, H. Development of a highly reproducible three-dimensional organotypic model of the oral mucosa. *Nat Protoc* **1**, 2012-2018 (2006).

9. Liu, X., *et al.* Chronic Inflammation-Related HPV: A Driving Force Speeds Oropharyngeal Carcinogenesis. *PLoS One* **10**, e0133681 (2015).

10. Zhong, R., *et al.* Notch1 Activation or Loss Promotes HPV-Induced Oral Tumorigenesis. *Cancer Res* (2015).

11. Visalli, G., *et al.* Higher levels of oxidative DNA damage in cervical cells are correlated with the grade of dysplasia and HPV infection. *J Med Virol* (2015).

12. De Marco, F., *et al.* Oxidative stress in HPV-driven viral carcinogenesis: redox proteomics analysis of HPV-16 dysplastic and neoplastic tissues. *PLoS One* **7**, e34366 (2012).

13. Sabit, H., Mallajosyula, S.S., MacKerell, A.D., Jr. & Swaan, P.W. Transmembrane domain II of the human bile acid transporter SLC10A2 coordinates sodium translocation. *J Biol Chem* **288**, 32394-32404 (2013).

14. Renner, O., *et al.* A variant of the SLC10A2 gene encoding the apical sodium-dependent bile acid transporter is a risk factor for gallstone disease. *PLoS One* **4**, e7321 (2009).

15. Vartiainen, M.K., Sarkkinen, E.M., Matilainen, T., Salminen, M. & Lappalainen, P. Mammals have two twinfilin isoforms whose subcellular localizations and tissue distributions are differentially regulated. *J Biol Chem* **278**, 34347-34355 (2003).

16. Ni, X., *et al.* Molecular cloning and characterization of a novel human Rab ( Rab2B) gene. *J Hum Genet* **47**, 548-551 (2002).

17. Hu, C., *et al.* The expression of ADAM23 and its correlation with promoter methylation in non-small-cell lung carcinoma. *Int J Exp Pathol* **92**, 333-339 (2011).

18. Poindexter, K., Nelson, N., DuBose, R.F., Black, R.A. & Cerretti, D.P. The identification of seven metalloproteinase-disintegrin (ADAM) genes from genomic libraries. *Gene* **237**, 61-70 (1999).

19. Benarroch, E.E. ADAM proteins, their ligands, and clinical implications. *Neurology* **78**, 914-920 (2012).

20. Owuor, K., *et al.* LGI1-associated epilepsy through altered ADAM23-dependent neuronal morphology. *Mol Cell Neurosci* **42**, 448-457 (2009).

21. Costa, E.T., *et al.* Intratumoral heterogeneity of ADAM23 promotes tumor growth and metastasis through LGI4 and nitric oxide signals. *Oncogene* **34**, 1270-1279 (2015).

22. Choi, J.-S., *et al.* Promoter hypermethylation of theADAM23gene in colorectal cancer cell lines and cancer tissues. *International Journal of Cancer* **124**, 1258-1262 (2009).

23. Verbisck, N.V., *et al.* ADAM23 negatively modulates alpha(v)beta(3) integrin activation during metastasis. *Cancer Res* **69**, 5546-5552 (2009).